Journal of Innate Immunity

Research Article

J Innate Immun 2024;16:354–366
DOI: 10.1159/000538625

Received: December 23, 2023
Accepted: March 26, 2024
Published online: June 8, 2024

TLR9-Dependent Activation by Inactivated Parapoxvirus Ovis in Murine Bone Marrow-Derived Dendritic Cells Is Associated with Specific Strain-Dependent Dendritic Cell Subsets

Yanqin Du[a, b] Hang Sun[a, c] Sonakshi Bhattacharjee[d] Alexander Birkmann[d] Ulf Dittmer[a] Mengji Lu[a]

[a]Institute for Virology, University Hospital Essen, University of Duisburg-Essen, Essen, Germany; [b]Department of Infectious Diseases, Union Hospital, Tongji Medical College, Huazhong University of Science and Technology, Wuhan, PR China; [c]Key Laboratory of Molecular Biology for Infectious Diseases, Ministry of Education, Institute for Viral Hepatitis, The Second Affiliated Hospital of Chongqing Medical University, Chongqing, PR China; [d]AiCuris Anti-infective Cures AG, Wuppertal, Germany

Keywords
Inactivated parapoxvirus ovis · Bone marrow-derived dendritic cells · Antigen presentation · Type I interferon · Proinflammatory cytokines

Abstract
Introduction: Inactivated parapoxvirus ovis (iPPVO) exerts strong immunomodulatory effects on innate immune cells, making it an attractive therapeutic candidate. However, little is known about the signaling pathways that are involved in iPPVO-induced immune responses. ***Methods:*** In this study, we systematically analyzed how different types of dendritic cells (DCs) react to iPPVO (Zylexis, strain D1701) in both BALB/c and C57BL/6 mice by flow cytometry and ELISAs, and investigated which signaling pathway is related to DC activation by Western blotting and protein profiling. ***Results:*** We demonstrated that bone marrow-derived conventional DCs (BM-cDCs) and bone marrow-derived plasmacytoid DCs (BM-pDCs) matured and secreted type I interferons in response to Zylexis stimulation in both mouse strains. Similarly, Zylexis promoted the secretion of IL-12/23p40 and TNF by pDCs. However, IL-12/23p40 and TNF secretion by cDCs were induced in BALB/c mice but not in C57BL/6 mice. Analyzing the underlying signaling pathways revealed that iPPVO-induced maturation of cDCs was Toll-like receptor 9 (TLR9) independent, while the maturation of pDCs partially depended on the TLR9 pathway. Moreover, the production of proinflammatory cytokines by cDCs and the secretion of IFN-α/β by pDCs partially depended on the TLR9 pathway in both mouse strains. Therefore, other signaling pathways seem to participate in the response of DCs to iPPVO, supported by protein profiling. ***Conclusion:*** Our data provide useful insights into the diversity of iPPVO sensors and their varying effects across different strains and species.

Introduction

Parapoxvirus ovis (PPVO), also known as orf virus, is an ovoid-shaped epitheliotropic double-stranded DNA virus (dsDNA) that belongs to the Poxviridae family. The

karger@karger.com
www.karger.com/jin

Correspondence to:
Mengji Lu, mengji.lu@uni-due.de

genome of PPVO is approximately 140 kb, and the size of the viral particle is approximately 200 nm. It is well known that both replication-competent and inactivated parapoxvirus ovis (iPPVO) exhibit immunomodulatory effects [1–3]. Increased production of proinflammatory cytokines and type I and type II interferons has been observed in innate immune cells from both mice [1] and humans [4, 5] after exposure to iPPVO. Moreover, iPPVO also promoted the maturation of dendritic cells (DCs) in vitro [6], which could subsequently enhance the antiviral adaptive immune response. In addition to these effects, iPPVO has shown antiviral effects against other viruses both in vivo and in vitro, including hepatitis B virus [4, 7], hepatitis C virus [3], and herpes simplex virus [8].

Activation of the innate immune response plays a critical role in priming the adaptive immune response, and DCs play a central role as a bridge between the innate and adaptive immune responses. As professional antigen-presenting cells, DCs can be broadly separated into two main types: conventional DCs (cDCs) and plasmacytoid DCs (pDCs) [9, 10]. cDCs ($CD11c^{+}CD11b^{+}B220^{-}$) exhibit typical functions such as antigen uptake, processing, and presentation, while pDCs ($CD11c^{low}CD11b^{-}B220^{+}$) are more potent in type I interferon production [9, 11]. DCs can be activated by pathogen-associated molecular patterns and thus orchestrate the expression of molecules associated with adaptive immunity. Toll-like receptor 9 (TLR9) is known to sense single-stranded DNA (ssDNA) containing unmethylated cytidinephosphateguanosine (CpG) [12]. A previous study showed that iPPVO-sensing receptor on pDCs is TLR9 [13]. However, an early study demonstrated that iPPVO elicits type I interferon production in cDCs via a TLR-independent pathway, while iPPVO-induced TNF production, MHCI, and CD86 expression in BMDCs required Myd88, which is used by several TLRs [6]. Therefore, it is still unclear whether the response of DCs to iPPVO depends on the TLR9 pathway.

In the present study, we systematically investigated how different types of DCs react to iPPVO (Zylexis, strain D1701) in both BALB/c and C57BL/6 mice and determined which signaling pathway is involved in this process. We found that a higher dose of Zylexis (1:10 dilution) induced maturation of both cDCs and pDCs in both mouse strains. Moreover, Zylexis enhanced the production of proinflammatory cytokines in cDCs from only BALB/c mice, although it obviously promoted the secretion of type I interferons by cDCs and pDCs in both mouse strains. Furthermore, Zylexis-induced maturation of cDCs did not depend on TLR9, while Zylexis-induced maturation of pDCs partially depended on the TLR9 pathway. Similarly, the production of proinflammatory cytokines and type I interferons by cDCs and pDCs in both mouse strains also partially depended on the TLR9 pathway. Protein profiling and Western blotting further showed that other signaling pathways participated in Zylexis-induced response in DCs.

Materials and Methods

Mice

C57BL/6 and BALB/c mice were purchased from Harlan Winkelmann Laboratories (Borchen, Germany) and maintained at the University Hospital of Essen according to the guidelines of the animal facility. Bone marrow from mice aged 8 to 16 weeks was used for all experiments.

Cell Culture

To generate bone marrow-derived pDCs (BM-pDCs), bone marrow cells were cultivated for 7 days in RPMI 1640 supplemented with 10% heat-inactivated fetal-inactivated fetal serum, 50 ng/mL FMS-like tyrosine kinase 3 ligand (Flt3L; Perpotech), 2 mM L-glutamine, 1 mM sodium pyruvate, 1% penicillin/streptomycin, 50 μM β-mercaptoethanol (Sigma-Aldrich), and 1% nonessential amino acids. To generate bone marrow-derived cDCs (BM-cDCs), bone marrow cells were cultivated for 7 days in RPMI 1640 supplemented with 10% heat-inactivated fetal-inactivated fetal serum, 2 mM L-glutamine, 1 mM sodium pyruvate, 1% penicillin/streptomycin, 50 μM β-mercaptoethanol (Sigma-Aldrich), and 1% nonessential amino acids in the presence of 20 ng/mL granulocyte-macrophage colony-stimulating factor (GM-CSF; Perpotech) and 20 ng/mL IL-4. Cells were then purified with CD11c microbeads prior to stimulation according to the manufacturer's instructions (Miltenyi Biotec).

Stimuli

A batch of Zylexis produced under commercial conditions was provided by AiCuris Ainti-infective Cures AG (Wuppertal Germany). This immunomodulatory stimulus consisted of freeze-dried iPPVO strain D1701 and L2 as a stabilizer. The dry pellet was resuspended in 1 mL of water for injection prior to being added to the culture medium. 1:10 dilution means adding 20 μL resuspended Zylexis into 180 μL medium in 96-well plate while 1:100 dilution means adding 2 μL resuspended Zylexis into 198 μL medium. As a control, cells were stimulated with TLR9 agonist CpG-ODN 1826 (0.5 μM). All stimuli were diluted in the appropriate medium prior to cell culture.

TLR9 Blocking

Cells were incubated with 0.5 μM ODN2088 for 3 h. Afterward, CpG-ODN1826 or Zylexis was added and incubated overnight.

Cytokine Detection Using ELISAs

BMDCs were stimulated with different agents for 24 h. Cell-free supernatants were collected, and TNF-α, IL-12/23p40 (Thermo Fisher Scientific, 88-7324-86; 88-7120-86), IFN-α (Invitrogen 421201), and IFN-β (Biolegend, 439407) levels were measured using ELISA kits according to the manufacturers' instructions.

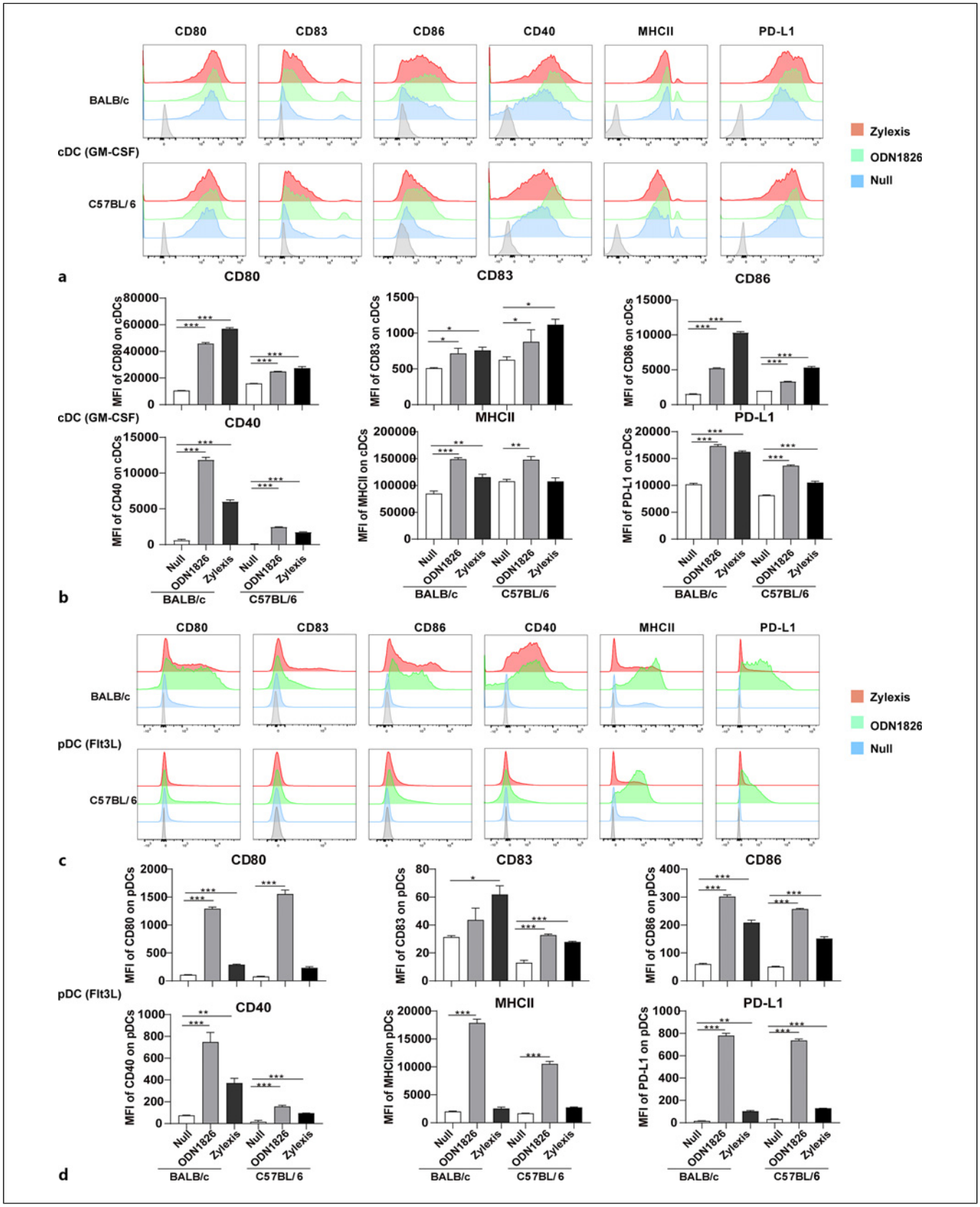

1

(For legend see next page.)

Flow Cytometry

Surface staining was performed by incubating the cells for 30 min in the dark at 4°C with the desired monoclonal antibody combination. For intracellular staining, the cells were fixed and permeabilized using the fixation/permeabilization buffer set (BD, Biosciences) for 30 min at 4°C and then stained with the desired antibody combinations. The monoclonal antibodies used for staining included anti-CD80, anti-CD83, anti-CD86, anti-CD40, anti-CD11c, anti-CD11b, anti-B220, anti-MHCII, anti-PD-L1, anti-IL-12, and anti-TNF antibodies (all from BD Bioscience, Biolegend, or eBioscience). The data were acquired on a FACS Canto II or FACS Symphony (BD, Bioscience) and analyzed with FlowJo software version 10.8 (Tree star). Cell debris and dead cells were excluded from the analysis based on forward/sideward scatter signals and staining with a fluorescent cell viability marker (eBioscience, Thermo Fisher Scientific).

Western Blotting

Western blot analysis was performed as previously described [14]. Briefly, cells were washed with PBS and lysed with 1× lysis buffer (Cell Signaling Technology, Beverly, MA, USA). Protein samples were resolved by SDS-PAGE and then electrotransferred to nitrocellulose membranes (Millipore, Germany). The membranes were incubated with the indicated primary antibodies overnight at 4°C after being blocked with 5% milk in 1X Tris-buffered saline with Tween 20. The following antibodies were used: STING, phospho-STING (Ser 365), c-GAS, TBK1/NAK, phospho-TBK1/NAK (Ser172), IRF-3, phospho-IRF-3 (Ser 396), Myd88, IRF-7, and phospho-IRF-7 (Ser 437) antibodies (all from Cell Signaling Technology). The membranes were washed 1 time with Tris-buffered saline with Tween 20 and incubated with a secondary peroxidase-affiniPure rabbit anti-mouse IgG antibody (Jackson ImmunoResearch Laboratories, West Grove, PA, USA) or a peroxidase-affiniPure goat anti-rabbit IgG antibody (Jackson ImmunoResearch Laboratories). Immunoreactive bands were visualized using an ECL system (GE Healthcare, Marlborough, MA, USA). The ratios of target proteins to β-actin were quantified by densitometry using ImageJ software.

Protein Profiling of cDCs

BM-cDCs from BALB/c mice were incubated with or without Zylexis. 24 h later, cells were collected, and proteins were extracted with scioExtract buffer (Sciomics) using the extraction SOPs. Then samples were analyzed on a scioDiscover antibody microarray (Sciomics) targeting 1,438 different proteins with 1,929 antibodies. Slide scanning was conducted using a Powerscanner (Tecan, Austria) with constant instrument laser power and PMT settings. The acquired raw data were analyzed using the linear models for the microarray data (LIMMA) package in R-Bioconductor after uploading the median signal intensities. For normalization, cyclic loess normalization was applied. For analysis of the samples, a one-factorial linear model was fitted via least squares regression with LIMMA, resulting in a two-sided t test or F test based on moderated statistics. All presented p values were adjusted for multiple testing by controlling the false discovery rate according to Benjamini and Hochberg. Proteins were defined as differentially expressed if $|\log FC| > 0.5$ and adjusted p value <0.05.

Statistical Analysis

Statistical analysis was performed with GraphPad Prism 8.0 (GraphPad Software, San Diego, CA, USA). Differences between two groups were determined by using Student's t test, and differences among multiple groups were evaluated by one-way analysis of variance (ANOVA). Data are presented as the mean ± standard error of the mean, and $p < 0.05$ was considered to indicate statistical significance. Significance is denoted with asterisks ($*p < 0.05$, $**p < 0.01$, $***p < 0.001$).

Results

Zylexis Promoted the Maturation of BMDC in Both Mouse Strains

Zylexis has been successfully used to generate vector vaccines in nonpermissive host species, such as horses and cats [15]. We first explored whether mouse DCs respond to Zylexis. The effects of Zylexis were dose dependent in splenocytes from BALB/c mice, as only a high concentration of Zylexis (1:10) promoted the production of TNF, IL-12, and IFN-α by total splenocytes (online suppl. Fig. S1A; for all online suppl. material, see https://doi.org/10.1159/000538625). Therefore, we chose a 1:10 dilution of Zylexis for the following experiments.

The expression of costimulatory molecules and major histocompatibility complex class II (MHC-II) on antigen-presenting cells directly correlates with their ability to present antigens to T cells and activate naïve T cells [16]. Previous study has shown that BALB/c and C57BL/6 mice express different TLRs in DCs, resulting in different reactivity to TLR Ligands [17]. Therefore, to analyze the phenotype of DCs responding to Zylexis in more detail, we stained for the costimulatory molecules CD80, CD83, CD86, CD40, MHC-II, and the coinhibitory molecule PD-L1 in DCs from both mouse strains. The TLR9 ligand CpG ODN, which has been characterized as a potent inducer of DC maturation and IFN-α production, was used as a control. On the one hand, upregulation of CD80, CD83, CD86, CD40, and PD-L1 was observed in cDCs (GM-CSF stimulated) from BALB/c and C57BL/6

Fig. 1. Zylexis induced the maturation of both BM-pDCs and BM-cDCs in both mouse strains. GM-CSF-generated BMDCs (**a**, **b**) and Flt3L-generated BMDCs (**c**, **d**) were purified with CD11c microbeads and then incubated with the TLR9 ligand ODN1826 or Zylexis for 24 h. Representative data (**a**) and summary of the expression (**b**) of CD80, CD83, CD86, CD40, MHCII, and PD-L1 on purified BM-cDCs. Representative data (**c**) and summary of the expression (**d**) of CD80, CD83, CD86, CD40, MHCII, and PD-L1 on purified BM-pDCs. The data shown represent the mean ± SEM of one of two representative experiments. $*p < 0.05$, $**p < 0.01$, $***p < 0.001$.

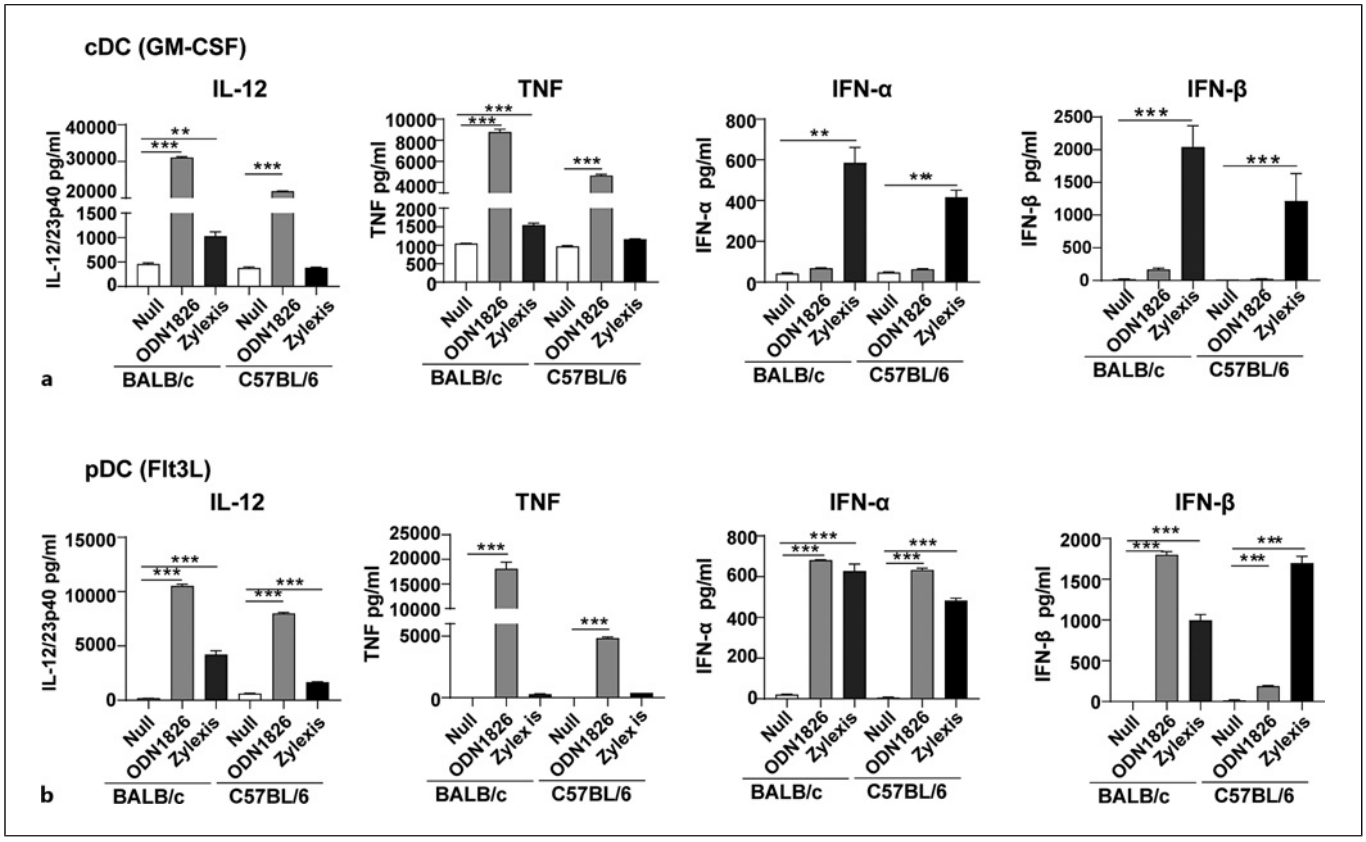

Fig. 2. Zylexis promoted the secretion of proinflammatory cytokines by cDCs in BALB/c mice but not in C57BL/6 mice. GM-CSF-generated BMDCs (**a**) and Flt3L-generated BMDCs (**b**) were purified with CD11c microbeads. **a**, **b** Purified BM-cDCs and BM-pDCs were stimulated with the TLR9 ligand ODN1826 or Zylexis for 24 h. The expression of IL-12/23p40, TNF, IFN-α, and IFN-β in supernatant was detected by ELISA. The data shown represent the mean ± SEM of one of two representative experiments. $*p < 0.05$, $**p < 0.01$, $***p < 0.001$.

mice in response to Zylexis (Fig. 1a, b). MHC-II was significantly upregulated in cDCs from BALB/c mice but not C57BL/6 mice after Zylexis stimulation (Fig. 1a, b). On the other hand, Zylexis also significantly changed the phenotype of the pDCs (Flt3L stimulated), causing marked upregulation of CD83, CD86, CD40, and PD-L1 in both mouse strains (Fig. 1c, d). Upregulation of CD80 was only observed in pDCs from BALB/c mice but not in C57BL/6 mice in response to Zylexis (Fig. 1c, d). Moreover, CpG ODN induced the expression of CD80, CD83, CD86, CD40, MHC-II, and PD-L1 on both cDCs and pDCs in both mouse strains. Interestingly, the levels of CD80, CD40, MHC-II, and PD-L1 in pDCs induced by CpG ODN were significantly higher than those in pDCs induced by Zylexis in both mouse strains (Fig. 1d). Altogether, these results suggest that Zylexis promoted the maturation of both cDCs and pDCs in both mouse strains.

Zylexis Promoted the Secretion of Type I Interferons and Proinflammatory Cytokines by BMDCs in Both Mouse Strains

In the next step, we explored whether the immunostimulatory effects of Zylexis were associated with the induction of proinflammatory cytokines and type I interferons. Upon Zylexis stimulation, both BM-cDCs (GM-CSF) and BM-pDCs (Flt3L) produced a large amount of IFN-α and IFN-β in both mouse strains (Fig. 2a, b). However, BM-cDCs (GM-CSF) from BALB/c mice but not those from C57BL/6 mice produced significantly more TNF and IL-12/23p40 after Zylexis stimulation (Fig. 2a). We also confirmed this result by flow cytometry, as the intracellular secretion of TNF and IL-12/23p40 by cDCs from BALB/c mice was significantly increased upon Zylexis treatment (online suppl. Fig. 2). As expected, CpG ODN induced the release of IFN-α and IFN-β in BM-pDCs but not by cDCs from both mouse strains while CpG ODN induced the release of TNF and IL-

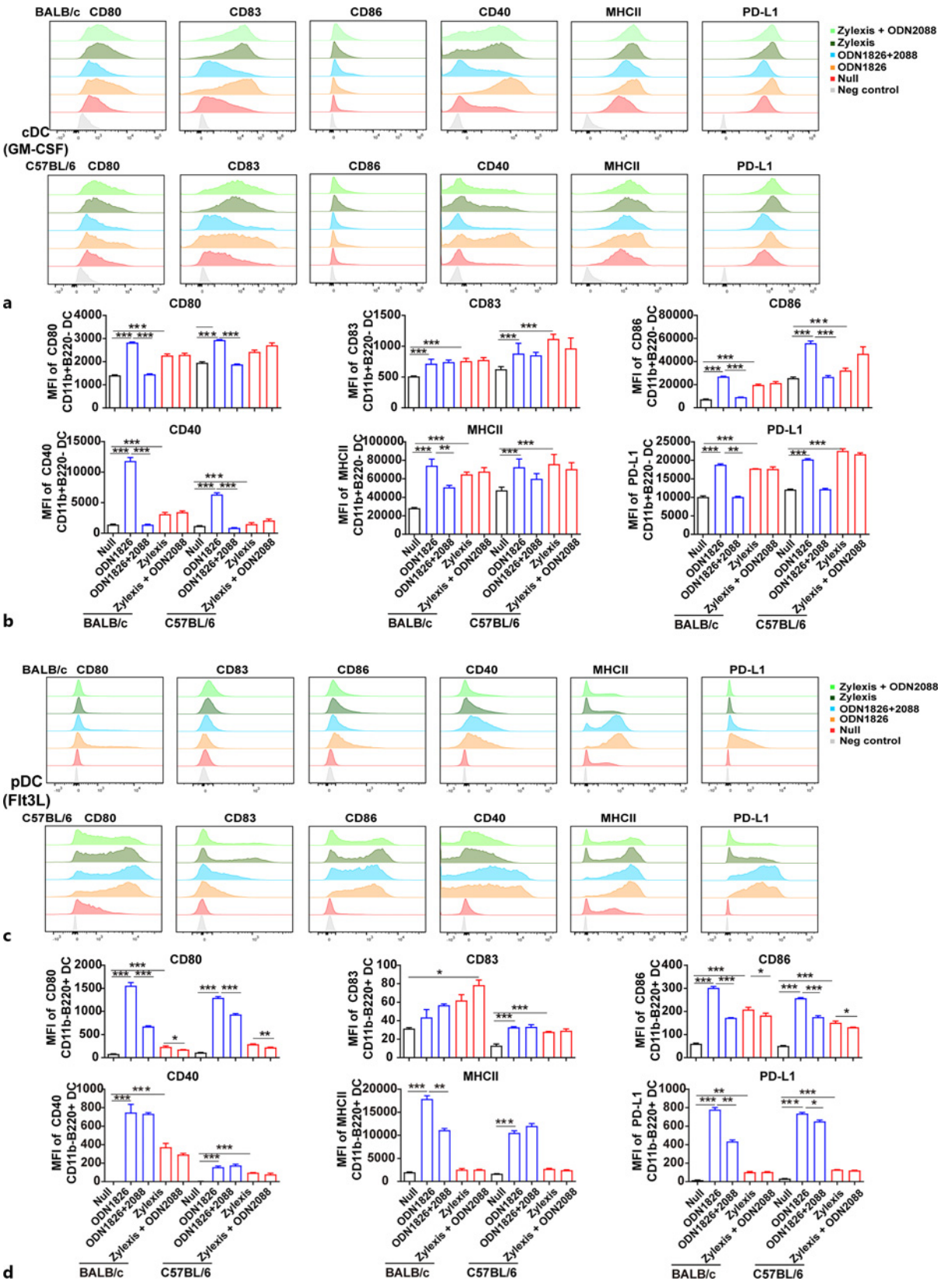

3

(For legend see next page.)

12/23p40 by BM-cDCs. This differs from the result obtained after Zylexis stimulation. Moreover, Zylexis-induced IL-12/23p40 but not TNF was significantly increased in BM-pDCs from both C57BL/6 and BALB/c mice (Fig. 2b).

The Maturation of pDCs but Not cDCs Partially Depended on the TLR9 Signaling Pathway upon Zylexis Stimulation

Previous studies have demonstrated that iPPVO-induced CD86 expression on BM-DCs is induced by TLR9 [6, 13]. To clarify whether Zylexis-induced upregulation of MHC-II, CD80, CD86, CD83, and CD40 required TLR9, the TLR9 antagonist ODN2088 was added before stimulation with Zylexis or the TLR9 ligand ODN1826. As expected, inhibiting TLR9 signaling diminished the expression of CD80, CD86, CD40, and PD-L1 induced by the TLR9 agonist ODN1826 in cDCs (GM-CSF) from both BALB/c and C57BL/6 mice. Surprisingly and unexpectedly, none of these markers induced by Zylexis displayed downregulation upon inhibition of TLR9 in cDCs (GM-CSF) in either mouse strain (Fig. 3a, b), suggesting that the maturation of cDCs does not depend on TLR9.

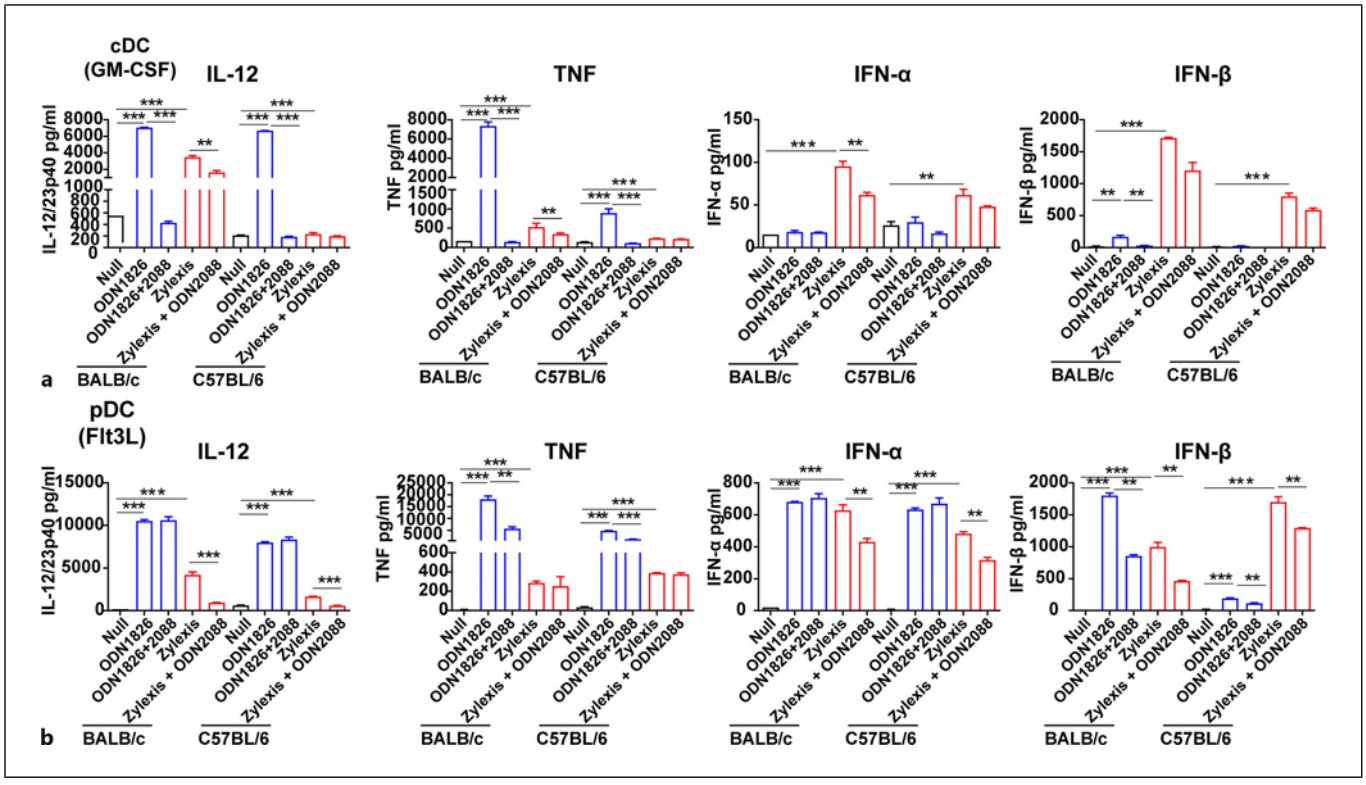

Fig. 4. Proinflammatory cytokine and type I interferon induction by Zylexis was partially dependent on TLR9 pathway. GM-CSF-generated BMDCs (**a**) and Flt3L-generated BMDCs (**b**) were purified with CD11c microbeads. **a**, **b** The purified BM-cDCs and BM-pDCs were incubated with or without the TLR9 antagonist ODN2088 for 3 h and then stimulated with the TLR9 ligand ODN1826 or Zylexis for another 24 h. After 24 h, the supernatant was collected. The expression of IL-12/23p40, TNF, IFN-α, and IFN-β was detected by ELISA. The data shown represent the mean ± SEM of one of two representative experiments. *$p < 0.05$, **$p < 0.01$, ***$p < 0.001$.

Fig. 3. The maturation of BM-cDCs induced by Zylexis was not dependent on the TLR9 pathway in either mouse strain. GM-CSF-generated BMDCs (**a**, **b**) and Flt3L-generated BMDCs (**c**, **d**) were purified with CD11c microbeads. The cells were incubated with or without the TLR9 antagonist ODN2088 for 3 h and stimulated with the TLR9 ligand ODN1826 or Zylexis for another 24 h. Representative data (**a**) and summary of the expression (**b**) of CD80, CD83, CD86, CD40, MHCII, and PD-L1 on purified BM-cDCs. Representative data (**c**) and summary of the expression (**d**) of CD80, CD83, CD86, CD40, MHCII, and PD-L1 on purified BM-pDCs. The data shown represent the mean ± SEM of one of two representative experiments. *$p < 0.05$, **$p < 0.01$, ***$p < 0.001$.

For comparison, we analyzed Zylexis-induced maturation of pDCs with or without TLR9 inhibition. Similar to cDCs (GM-CSF), blocking TLR9 with ODN2088 suppressed the expression of CD80, CD86, MHC-II, and PD-L1 induced by ODN1826 in pDCs (Flt3L) from both BALB/c and C57BL/6 mice. In line with this, Zylexis-induced CD80 and CD86 expression in pDCs was downregulated after blocking TLR9, which is in contrast to the results observed in cDCs (GM-CSF). However, the TLR9 antagonist did not influence the expression of CD40, CD83, MHCII, and PD-L1 triggered by Zylexis in pDCs from the two mouse strains (Fig. 3c, d). This implied that the maturation of pDCs after iPPVO stimulation partially depends on TLR9.

Zylexis-Induced Type I IFN and Proinflammatory Cytokine Production by cDCs and pDCs Was Partially Mediated by TLR9

We observed that Zylexis induced IFN-α/β, IL-12/23p40, and TNF-α production in cDCs (GM-CSF), especially in BALB/c mice. Therefore, we wanted to investigate whether cytokine production by cDCs was also dependent on the TLR9 pathway. ODN1826-triggered IL-12/23p40, TNF-α, and IFN-β production by cDCs was diminished after inhibiting TLR9 by ODN2088 preincubation (Fig. 4a, b). However, the TLR9 antagonist did not influence the production of IFN-α triggered by ODN1826. Inhibiting TLR9 also significantly suppressed the IFN-α/β, IL-12/23p40, and TNF-α production induced by Zylexis in cDCs from BALB/c mice. In line with the results obtained in cDCs (GM-CSF), pDCs (Flt3L) produced less IFN-α/β and IL-12/23p40 in response to Zylexis in both mouse strains after inhibiting the TLR9 signaling pathway (Fig. 4a, b). This is also consistent with a previous study, which identified TLR9 as the main PPVO-sensing receptor triggering the activation of pDCs [13]. Nevertheless, the levels of these cytokines were still significantly higher than those in the control group without TLR ligand stimulation. This suggested that the production of the cytokines IFN-α/β, IL-12/23p40, and TNF-α by cDCs also partially depended on TLR9 signaling.

STING and Other Pattern Recognition Receptor Signaling Pathways Participate in Zylexis-Induced cDC Activation

We observed that the activation of cDCs and pDCs partially depended on TLR9. As cDCs (GM-CSF) from BALB/c mice exhibited strong activation upon Zylexis stimulation, we chose cDCs from BALB/c mice for further mechanistic investigation. Cyclic GMP-AMP (cGAMP) synthase (cGAS) is a cytosolic DNA sensor that activates the adaptor STING. To explore whether Zylexis induced DC activation through the cGAS-STING pathway, we analyzed the expression of proteins in the reactive STING pathway, including STING, c-GAS, TBK1/NAK, IRF-3, and IRF-7, by Western blotting. As shown in Figure 5a, the levels of phosphorylated TBK1/NAK and phosphorylated IRF-3 significantly increased in ODN1826- and Zylexis-stimulated cDCs. However, pSTING was not enhanced in cDCs after Zylexis stimulation (Fig. 5a). Moreover, pTBK-1 and pIRF3 are also involved in TLR9-MyD88 and signaling RIG-I signaling. To confirm whether other signaling pathways are involved in Zylexis-induced cDC activation in BABL/c mice, we compared the protein profiles of cDCs from BALB/c mice upon Zylexis stimulation with those of the control group. A total of 101 proteins showed differential abundance between Zylexis samples and control samples, as summarized in the volcano plot and heatmap (Fig. 5b, c). Among the 101 proteins, the levels of 42 proteins were significantly higher in Zylexis-stimulated cDCs than in the control group. Furthermore, we analyzed the functional annotations of differentially expressed proteins via KEGG pathways (Table 1). We found that these 42 proteins were involved in the PI3K-Akt signaling pathway, JAK-STAT signaling pathway, TLR signaling pathway, MAPK family signaling cascades, NOD-like receptor signaling pathway, retinoic acid-inducible gene I (RIG-I)-like receptor signaling pathway, and so on. The PI3K-Akt signaling pathway is related to mammalian enzyme-related receptors involved in transducing signals or biological processes such as cell development, differentiation, cell survival, protein synthesis, and metabolism [18]. The RIG-I-like receptor is a key sensor of virus infection, mediating the transcriptional induction of type I interferons [19]. NOD-like receptors are involved in the formation of inflammasomes, which mediate cleavage of the proinflammatory cytokines IL-1β and IL-18 into their active and secreted forms [20]. This diversity might be due to the complex components of Zylexis particles.

Discussion

IPPVO has been shown to exhibit immunomodulatory effects in animals both in vivo and in vitro, leading to antiviral activity against a range of different viruses.

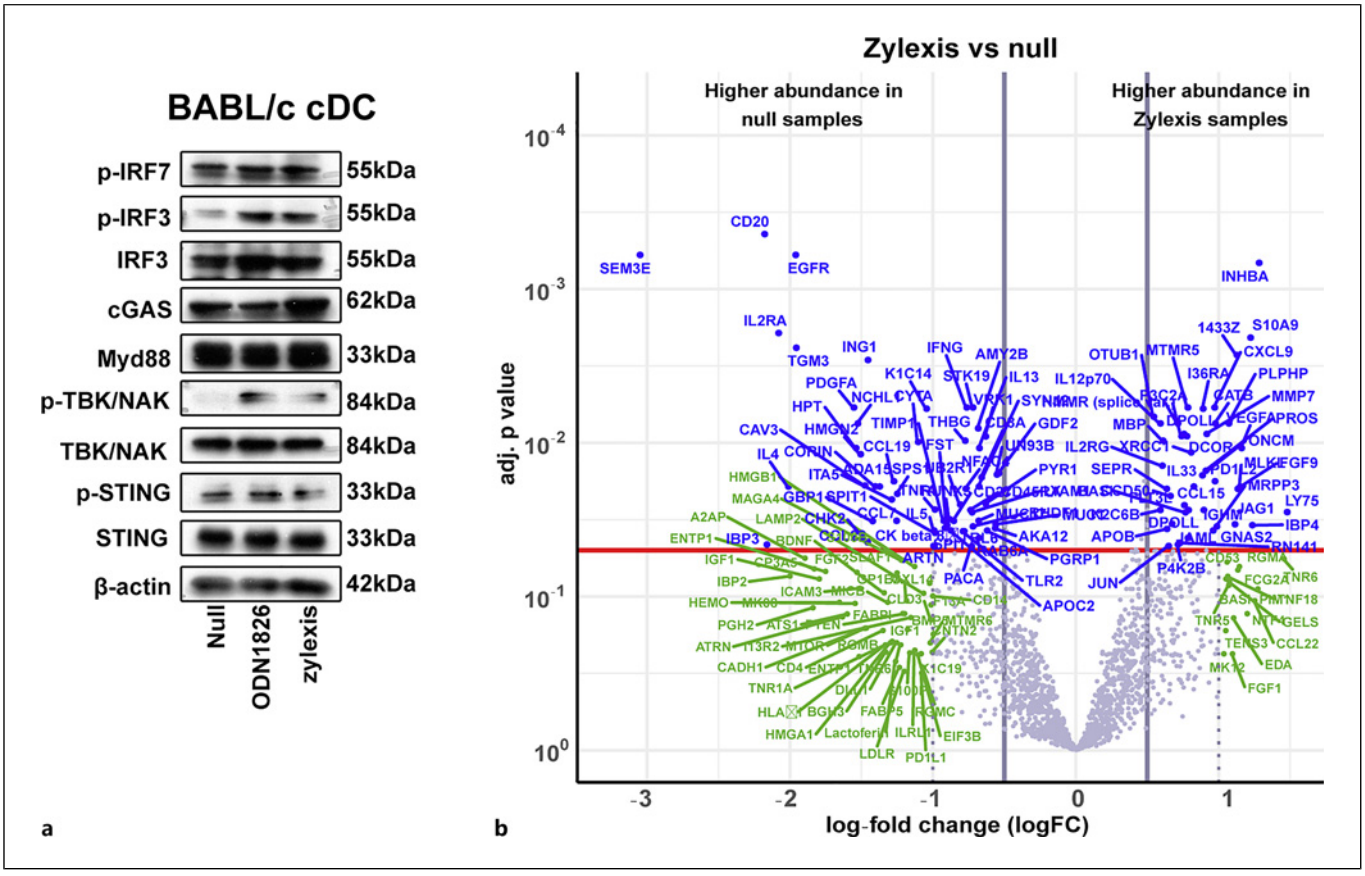

5

(Figure continued on next page.)

However, little is known about the signaling pathways that are involved in iPPVO-induced immune responses. Here, we used professional antigen-presenting cells, DCs, and systematically analyzed how different types of DCs from both BALB/c and C57BL/6 mice react to iPPVO in vitro and investigated which signaling pathway is related to activation during Zylexis stimulation. Zylexis promoted the secretion of type I interferons by cDCs and pDCs and IL-12/23p40 and TNF by pDCs from both mouse strains, while IL-12/23p40 and TNF production in cDCs was induced only in cells derived from BALB/c mice. Furthermore, Zylexis-induced maturation of cDCs did not depend on TLR9, while Zylexis-induced maturation of pDCs partially depended on the TLR9 pathway. Similarly, the production of proinflammatory cytokines and type I interferons by cDCs and pDCs in both mouse strains also partially depended on the TLR9 pathway. Protein profiling and Western blotting further suggested that other pattern recognition receptor signaling pathways participated in the Zylexis-induced response in DCs.

A previous study showed that both cDCs and pDCs substantially contribute to IFN-α/β production upon stimulation by iPPVO in C57BL/6 mice [6]. In the present study, we demonstrated that Zylexis induced IFN-α/β production by both cDCs and pDCs from two mouse strains, which is more obvious in cells derived from BALB/c mice. This demonstrated that Zylexis induced a divergent response in the same cells from different mouse strains. The role of pDCs producing IFN-α/β in response to iPPVO and viral encounters has been studied extensively in C57BL/6 mice [13, 21]. The genome of iPPVO comprises dsDNA [22]. Therefore, TLR9, which senses single-stranded CpG DNA motifs, is likely to be involved in the induction of IFN-α/β production in pDCs by iPPVO. In line with this, von Buttlar et al. [13] identified that the induction of IFN-α/β production by PPVO in pDCs depended on TLR9. Consistently, in our present study, the production of

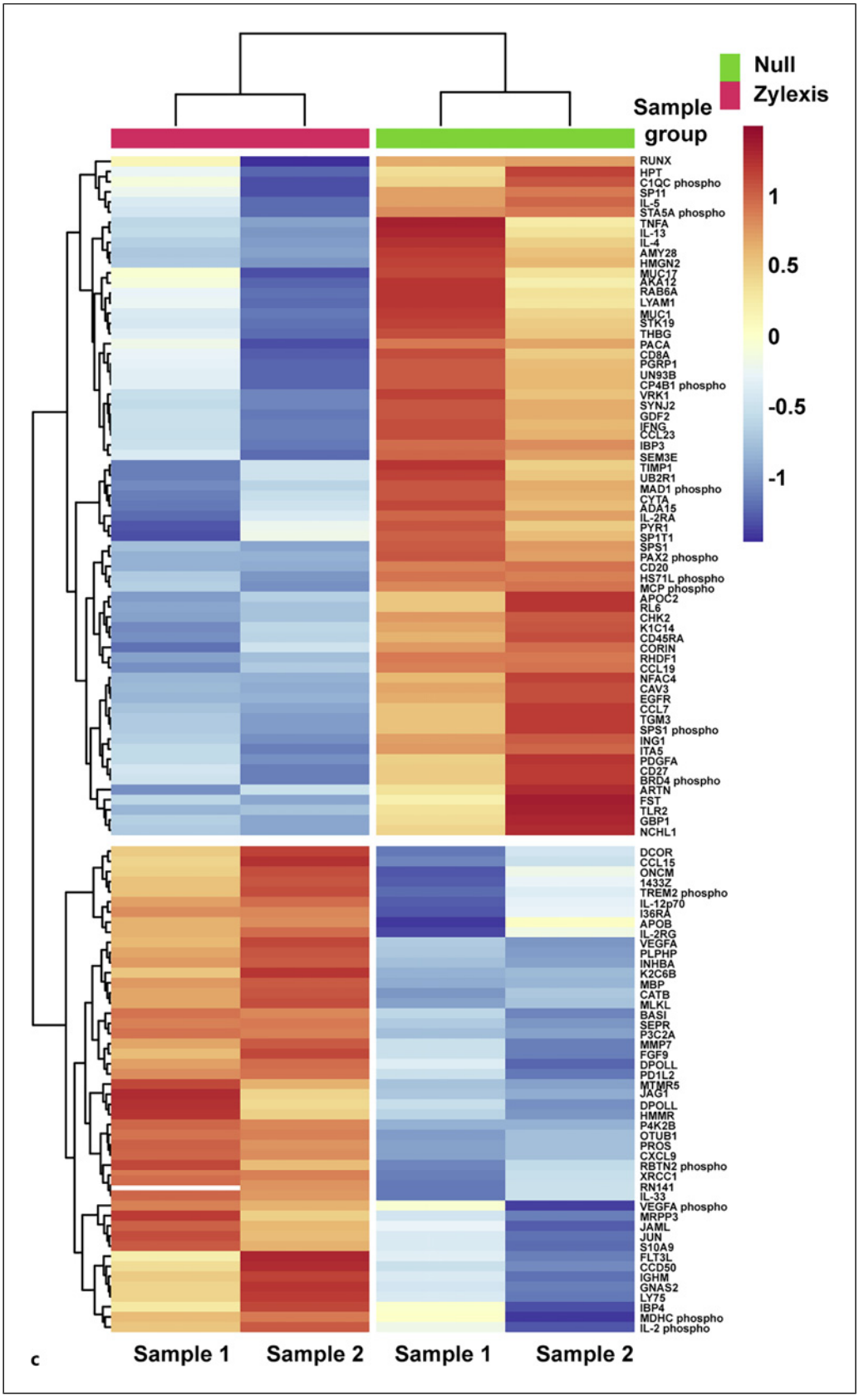

5

(For legend see next page.)

Table 1. Selected KEGG pathways related to proteins with differential abundance and phosphorylation in Zylexis versus null

Pathway ID	Pathway description	Protein counts	Proteins
hsa04151	PI3K-Akt signaling pathway	9	COL1A1, FGF1, FGF9, FLT3LG, GNAS, NTF4, OSM, VEGFA, YWHAZ
hsa04630	JAK-STAT signaling pathway	4	IL-12A, IL-2, IL-2RG, OSM, PIM1
hsa04620	TLR signaling pathway	5	CD40, CXCL9, IL-12A, JUN, MAPK12
hsa04010	MAPK family signaling cascades	8	FGF1, FGF9, FLT3LG, HSPA1L, JUN, VEGFA, MAPK12, NTF4
hsa04668	TNF signaling pathway	4	JAG, JUN, MLKL, TNF
hsa04064	NK-kappa B signaling	3	CD40, CXCL12, EDA
hsa04621	NOD-like receptor signaling pathway	3	CTSB, JUN, MAPK12
hsa04622	RIG-I-like receptor signaling pathway	3	IL-12A, MAPK12

Proteins that indicated a higher protein abundance in Zylexis samples were shown in the table.

IFN-α/β in Zylexis-exposed pDCs also partially depended on the TLR9 signaling pathway. However, the role of cDCs in IFN-α/β production is not clear during viral infection. A previous study demonstrated that the production of IFN-α/β by iPPVO-induced cDCs did not require Myd88 and TRIF, indicating that receptors other than the currently known TLRs are involved in this process [6].

A TLR-independent DNA sensing mechanism was reported to be involved in response to microbial and host nucleic acids [23]. For instance, primary human endothelial cells mount a robust IFN-I response to human cytomegalovirus via the cGAS/STING/IRF3 pathway [24]. Recent studies have also shed significant light on the mechanism of RIG-I-like receptor (RLR) activation during DNA virus infection. The coding and noncoding RNAs produced during DNA virus infection may contain the chemical moieties recognized by RLRs [25]. In line with these findings, in the present study, the levels of phosphorylated TBK1/NAK and phosphorylated IRF-3 were higher in Zylexis-exposed cDCs, indicating that the cGAS/STING/IRF3 pathway might be involved in Zylexis recognition (Fig. 5a).

Interestingly, we found that increased secretion of TNF-α and IL-12/23p40 by cDCs in response to iPPVO occurred in BALB/c mice but not in C57BL/6 mice (Fig. 2a). A previous study showed that $CD8^+$ DCs are the major producers of IL-12p70 in response to TLR stimulation, particularly TLR9 [26]. The higher percentage of $CD8^+$ cDCs out of cDCs in BALB/c mice than those in C57BL/6 mice (online suppl. Fig. 3) may partially explain the relatively higher production of IL-12 in cDCs from BALB/c mice compared to those from C57BL/6 mice. Moreover, DCs isolated from the spleen of naïve C57BL/6 mice preferentially expressed TLR9 mRNA, whereas DCs from naïve BALB/c mice strongly expressed TLR2, -4, -5, and -6 mRNA [17]. Furthermore, BMDCs from different mouse strains displayed differences in their responses to pathogens. For instance, compared to BMDCs from BALB/c mice, BMDCs from DBA/2 mice upregulated TLR3 and TLR4 gene expression and secretion of IL-12 in response to Coccidioides posadasii [27]. Therefore, the divergent production of TNF-α and IL-12/23p40 by cDCs from BALB/c mice and C57BL/6 mice may also be related to differential

Fig. 5. Other signaling pathways were involved in the Zylexis-induced responses. BM-cDCs from BALB/c mice were stimulated with or without Zylexis for 24 h. The cells were collected, and total protein was extracted. **a** The expression of Myd88 and the components of the STING pathway were detected by Western blotting. **b**, **c** Protein profiles of cDCs were determined with a scioDiscover antibody microarray (Sciomics) targeting 1,438 different proteins with 1,929 antibodies. **b** The volcano plot revealed distinct abundance variations between Zylexis samples and null samples. The significance level (adj. p value = 0.05) is indicated as a horizontal red line. The logFC cutoffs are indicated as vertical lines. Proteins with a positive logFC had a higher abundance in Zylexis samples, and proteins with a negative value had a higher abundance in null samples. Proteins with $|\log FC| > 0.5$ and a significant adj. p value are defined as differentially expressed and displayed in blue. **c** Heatmap displaying the relative expression of proteins identified as differentially expressed between two groups.

expression of pattern recognition receptors between the two mouse strains, which may thus lead to discrepant responses to Zylexis.

In our study, Zylexis and ODN1826 displayed several similarities and differences. Zylexis is a kind of iPPVO, which is a double-stranded DNA (dsDNA) virus, while ODN1826 belongs to ssDNA. Both Zylexis and ODN1826 can induce the maturation of cDCs and pDCs. However, the levels of co-stimulatory molecules induced by these two stimuli were quite different. The expression of CD80, CD86, CD40, MHCII, and PD-L1 in pDCs induced by ODN1826 was significantly higher than those induced by Zylexis, while CD80 and CD86 in cDCs induced by ODN1826 was even lower than those induced by Zylexis. Moreover, both ODN1826 and Zylexis induced the production of proinflammatory cytokines and type I IFN by cDCs. Of note, type I IFN produced by cDCs induced by Zylexis was significantly higher than that induced by ODN1826. This is in line with the previous study that iPPVO elicits type I IFN production by cDC in TLR-independent pathways [6].

The present study demonstrated that Zylexis-induced antigen-presenting cells maturation correlated with increased expression of costimulatory molecules on both cDCs and pDCs (Fig. 1). The expression of these molecules on Zylexis-exposed pDCs was partially suppressed after inhibiting the TLR9 pathway. However, MHC-II and costimulatory molecules induced by Zylexis on cDCs did not depend on TLR9, suggesting that Zylexis activates cDCs in a different way than pDCs. Of note, TLR9 antagonist ODN2088 disrupts the colocalization of CpG ODNs with TLR9 in endosomal vesicles without affecting cellular binding and uptake. Therefore, it does not completely block TLR9. This can also be verified by no change of MHC-II in pDCs from C57BL/6 and CD40 in pDCs from C57BL/6 and BALB/c mice upon ODN2088 suppression before ODN1826 stimulation (Fig. 3c, d). This is a limitation of this study. Previously, Siegemund et al. [6] demonstrated that TLR2 and TLR4 were not required for iPPVO-triggered Myd88-dependent TNF-α and IL-12/23p40 production or CD86 upregulation, indicating that there are other signaling pathways related to iPPVO-induced DC activation. In line with this, in our study, we found that 42 upregulated proteins in Zylexis-exposed cDCs were related to the PI3K-Akt, JAK-STAT, TLR, MAPK family, NOD-like receptor, and RLR signaling pathways (Fig. 5b, c). However, further studies should be performed to confirm the iPPVO-sensing receptor in cDCs. Moreover, the detailed mechanism by which cDCs respond to Zylexis differently in BALB/c and C57BL/6 mice should be investigated.

In conclusion, our study demonstrated that TLR9-dependent activation of BMDCs by Zylexis involves strain-specific dendritic subsets. Our results provide important insights that there are different iPPVO sensors and that iPPVO has different effects in different strains and different species.

Acknowledgment

We thank Ms. Thekla Kemper (Institute for Virology, University Hospital Essen) for excellent technical Support.

Statement of Ethics

This study was granted an exemption from the need for ethical approval by the Ethics Committee of University Hospital Essen.

Conflict of Interest Statement

The authors have no conflicts of interest to declare.

Funding Sources

This study was supported by a scholarship of Medical Faculty of University of Duisburg-Essen, a grant of Deutsche Forschungsgemeinschaft (RTG 1949/2), and a grant of National Natural Science Foundation of China (82302508).

Author Contributions

Y.D. designed the study scheme, collected and analyzed data, and drafted the manuscript. H.S. performed part of the experiments and analyzed the data. S.B. and A.B. participated in coordination of the study and revised the manuscript. M.L. and U.D. conceptualized this manuscript and revised the manuscript. All authors read and approved the final manuscript.

Data Availability Statement

The data that support the findings of this study are not publicly available but are available from the corresponding author (M.L.) upon reasonable request.

References

1 Anziliero D, Weiblen R, Kreutz LC, Spilki F, Flores EF. Inactivated Parapoxvirus ovis induces a transient increase in the expression of proinflammatory, Th1-related, and autoregulatory cytokines in mice. Braz J Med Biol Res. 2014;47(2):110–8. https://doi.org/10.1590/1414-431X20133358

2 Friebe A, Friederichs S, Scholz K, Janssen U, Scholz C, Schlapp T, et al. Characterization of immunostimulatory components of Orf virus (Parapoxvirus ovis). J Gen Virol. 2011;92(Pt 7):1571–84. https://doi.org/10.1099/vir.0.028894-0

3 Anziliero D, Kreutz LC, Flores EF, Weiblen R. Effects of inactivated Parapoxvirus ovis on cellular and humoral events of the innate immune response in mice. Cell Immunol. 2014;289(1–2):36–41. https://doi.org/10.1016/j.cellimm.2014.03.005

4 Weber O, Schlemmer KH, Hartmann E, Hagelschuer I, Paessens A, Graef E, et al. Inhibition of human Hepatitis B Virus (HBV) by a novel non-nucleosidic compound in a transgenic mouse model. Antiviral Res. 2002;54(2):69–78. https://doi.org/10.1016/s0166-3542(01)00216-9

5 Friebe A, Siegling A, Friederichs S, Volk HD, Weber O. Immunomodulatory effects of inactivated parapoxvirus ovis (Orf virus) on human peripheral immune cells: induction of cytokine secretion in monocytes and Th1-like cells. J Virol. 2004;78(17):9400–11. https://doi.org/10.1128/JVI.78.17.9400-9411.2004

6 Siegemund S, Hartl A, von Buttlar H, Dautel F, Raue R, Freudenberg MA, et al. Conventional bone marrow-derived dendritic cells contribute to toll-like receptor-independent production of alpha/beta interferon in response to inactivated Parapoxvirus ovis. J Virol. 2009;83(18):9411–22. https://doi.org/10.1128/JVI.02362-08

7 Paulsen D, Weber O, Ruebsamen-Schaeff H, Tennant BC, Menne S. AIC649 induces a Bi-Phasic treatment response in the woodchuck model of chronic Hepatitis B. PLoS One. 2015;10(12):e0144383. https://doi.org/10.1371/journal.pone.0144383

8 Weber O, Siegling A, Friebe A, Limmer A, Schlapp T, Knolle P, et al. Inactivated Parapoxvirus ovis (Orf virus) has antiviral activity against Hepatitis B virus and herpes simplex virus. J Gen Virol. 2003;84(Pt 7):1843–52. https://doi.org/10.1099/vir.0.19138-0

9 Segura E. Review of mouse and human dendritic cell subsets. Methods Mol Biol. 2016;1423:3–15. https://doi.org/10.1007/978-1-4939-3606-9_1

10 Macri C, Pang ES, Patton T, O'Keeffe M. Dendritic cell subsets. Semin Cell Dev Biol. 2018;84:11–21. https://doi.org/10.1016/j.semcdb.2017.12.009

11 Brawand P, Fitzpatrick DR, Greenfield BW, Brasel K, Maliszewski CR, De Smedt T. Murine plasmacytoid pre-dendritic cells generated from Flt3 ligand-supplemented bone marrow cultures are immature APCs. J Immunol. 2002;169(12):6711–9. https://doi.org/10.4049/jimmunol.169.12.6711

12 Lind NA, Rael VE, Pestal K, Liu B, Barton GM. Regulation of the nucleic acid-sensing Toll-like receptors. Nat Rev Immunol. 2022;22(4):224–35. https://doi.org/10.1038/s41577-021-00577-0

13 von Buttlar H, Siegemund S, Buttner M, Alber G. Identification of Toll-like receptor 9 as parapoxvirus ovis-sensing receptor in plasmacytoid dendritic cells. PLoS One. 2014;9(8):e106188. https://doi.org/10.1371/journal.pone.0106188

14 Lin Y, Wu C, Wang X, Liu S, Kemper T, Li F, et al. Synaptosomal-associated protein 29 is required for the autophagic degradation of Hepatitis B virus. FASEB J. 2019;33(5):6023–34. https://doi.org/10.1096/fj.201801995RR

15 Ons E, Van Brussel L, Lane S, King V, Cullinane A, Kenna R, et al. Efficacy of a Parapoxvirus ovis-based immunomodulator against equine herpesvirus type 1 and Streptococcus equi equi infections in horses. Vet Microbiol. 2014;173(3–4):232–40. https://doi.org/10.1016/j.vetmic.2014.07.015

16 Chudnovskiy A, Pasqual G, Victora GD. Studying interactions between dendritic cells and T cells in vivo. Curr Opin Immunol. 2019;58:24–30. https://doi.org/10.1016/j.coi.2019.02.002

17 Liu T, Matsuguchi T, Tsuboi N, Yajima T, Yoshikai Y. Differences in expression of toll-like receptors and their reactivities in dendritic cells in BALB/c and C57BL/6 mice. Infect Immun. 2002;70(12):6638–45. https://doi.org/10.1128/IAI.70.12.6638-6645.2002

18 Sharma A, Mehan S. Targeting PI3K-AKT/mTOR signaling in the prevention of autism. Neurochem Int. 2021;147:105067. https://doi.org/10.1016/j.neuint.2021.105067

19 Rehwinkel J, Gack MU. RIG-I-like receptors: their regulation and roles in RNA sensing. Nat Rev Immunol. 2020;20(9):537–51. https://doi.org/10.1038/s41577-020-0288-3

20 Platnich JM, Muruve DA. NOD-like receptors and inflammasomes: a review of their canonical and non-canonical signaling pathways. Arch Biochem Biophys. 2019;670:4–14. https://doi.org/10.1016/j.abb.2019.02.008

21 Fitzgerald-Bocarsly P, Dai J, Singh S. Plasmacytoid dendritic cells and type I IFN: 50 years of convergent history. Cytokine Growth Factor Rev. 2008;19(1):3–19. https://doi.org/10.1016/j.cytogfr.2007.10.006

22 Cottone R, Buttner M, Bauer B, Henkel M, Hettich E, Rziha HJ. Analysis of genomic rearrangement and subsequent gene deletion of the attenuated Orf virus strain D1701. Virus Res. 1998;56(1):53–67. https://doi.org/10.1016/s0168-1702(98)00056-2

23 Wagner H, Bauer S. All is not Toll: new pathways in DNA recognition. J Exp Med. 2006;203(2):265–8. https://doi.org/10.1084/jem.20052191

24 Lio CW, Mcdonald B, Takahashi M, Dhanwani R, Sharma N, Huang J, et al. CGAS-STING signaling regulates initial innate control of cytomegalovirus infection. J Virol. 2016;90(17):7789–97. https://doi.org/10.1128/JVI.01040-16

25 Zhao Y, Karijolich J. Know thyself: RIG-I-Like receptor sensing of DNA virus infection. J Virol. 2019;93(23):e01085. https://doi.org/10.1128/JVI.01085-19

26 Hochrein H, Shortman K, Vremec D, Scott B, Hertzog P, O'Keeffe M. Differential production of IL-12, IFN-alpha, and IFN-gamma by mouse dendritic cell subsets. J Immunol. 2001;166(9):5448–55. https://doi.org/10.4049/jimmunol.166.9.5448

27 Awasthi S, Magee DM. Differences in expression of cell surface co-stimulatory molecules, Toll-like receptor genes and secretion of IL-12 by bone marrow-derived dendritic cells from susceptible and resistant mouse strains in response to Coccidioides posadasii. Cell Immunol. 2004;231(1–2):49–55. https://doi.org/10.1016/j.cellimm.2004.11.006

DOI: 10.1159/000538625
URN: urn:nbn:de:hbz:465-20250106-160134-7